

Achieving Controllable and Reversible Snap-Through in Pre-strained Strips of Liquid Crystalline Elastomers

James T. Waters ^a and Anna C. Balazs ^{a*}

^a Department of Chemical and Petroleum Engineering, University of Pittsburgh
Pittsburgh, PA 15213

Supporting Information

I. Energy released by a Snap Through

To estimate how much energy the strip releases as it undergoes snap through, we compute the deformation energy of the strip as a function of time by using the expressions for the free energy given in Eqs. 1 and 2 and snapshots from the finite element simulation (to visualize the conformation of the system). In Fig. S1, the energy associated with the deformation of the strip is plotted in terms of energy density (J/cm^3) to provide a result that is independent of the width of the strip. This deformation energy is plotted for three different light intensities: $15 \text{ mW}/\text{cm}^2$, $30 \text{ mW}/\text{cm}^2$, and $60 \text{ mW}/\text{cm}^2$. The energy at $t=0$, when the light is introduced, is non-zero, reflecting the energy cost of the initial strain in the strip. For the lowest of these light intensities (blue line), the system is pushed into a higher energy state but fails to undergo snap-through. At $30 \text{ mW}/\text{cm}^2$ (orange line), the system is driven into a more elevated state, which is only temporarily stable. The abrupt drop beyond 100 time steps coincides with the switch from downward-buckled to upward-buckled state that occurs to relieve the stress. The difference between the energy of these two states allows us to estimate the energy released by the snap-through, yielding a value of $2.7 \times 10^{-3} \text{ J}/\text{cm}^3$. For the highest light intensity shown here (yellow line), the system undergoes snap-through at relatively early times, while the free energy is still rising due to the isomerization induced in the material. The energy released in this case is $3.3 \times 10^{-3} \text{ J}/\text{cm}^3$, which is comparable in magnitude to the lower intensity case.

II. Effect of Shifting the Position of Light Along the Long Axis of the Strip

Figure 6 (in the main text) reveals the asymmetric process by which the strip under strain transitions from one buckled state to the other. Here, the initial conditions and the incident light are symmetric about the center of the long axis of the strip. Prior to the snap through, the middle of the illuminated strip shifts arbitrarily to the left or right. With a shift in the position of the incident light to one side or the other, the snap-through behavior persists across a range of light positions. Figure S2A shows the phase map for the system as a function of aperture size and position of the center of the light. The blue triangles mark cases where snap-through occurs for a constant light intensity of $60 \text{ mW}/\text{cm}^2$. Obtained by using the semi-analytical model, the latter phase map shows that the snap-through behavior in Fig. 3 is robust for small displacements along the length of the strip. The asymmetry introduced by offsetting the incident light also extends the area for which snap through occurs, which can be inferred from Fig. S2A

Figure 6B indicates that snap-through failed to occur in the finite element model for an elastomer when the isomerized region was fixed in the material frame. The phase diagram obtained from the semi-analytic model is plotted in Fig. S2B as a function of the size of the illuminated patch in the strip and location of the center of the illuminated patch. We use “patch” size and location to distinguish the dual-phase case where snap through failed to occur in the finite element

model. (As defined in the main text, dual-phase refers to a case where the nematic to isotropic has occurred in one portion of the material.) The plot marks the range of positions and aperture sizes where snap-through is expected to occur for light intensity of 60 mW/cm^2 . Unlike the corresponding case in Fig. S2A, the phase diagram now indicates that the symmetric system does not undergo snap through. This behavior reflects the result in Fig. 6B where snap-through did not occur for an active, illuminated region symmetric about the center. The plots reveal that the existence of a trade-off; some small degree of asymmetry is desirable to induce a transition from one buckled state to another. The region subject to a light-induced curvature, however, should include the middle of the strip and exclude the edges of the strip to distinguish the free energy of the upward buckled state from that of the downward buckled state.

This prediction from our semi-analytical model was then corroborated with a set of finite element simulations, which demonstrated snap-through occurring for material conditions with asymmetry. Curves representing the final shape of the buckled strip are displayed in Fig. S3, for an active patch length of 0.6 the relaxed length and an incident intensity of 60 mW/cm^2 . For an active patch offset by -0.2 of the strip length from the center, the region undergoing a phase transition will extend from -0.5 to 0.1 in the normalized material frame coordinates, meaning it extends from one edge of the strip beyond the center of the strip. In this case, the induced curvature does not favor upward buckling and the strip is trapped in the downward buckled state (blue curve). When the active region is moved toward the center (-0.1 and -0.05 , orange and yellow curves) the induced curvature at the center of the strip results in a lower free energy in the upward buckled state and the asymmetry is sufficient for the system to transition between the two states. As the active region approaches the center, at a position of -0.025 in the normalized material frame coordinates, upward buckling is energetically favorable but the system is trapped in the downward-buckled state (purple curve). The appearance and disappearance of snap-through behavior as the active region is shifted corresponds to the separated regions on either side of the center where snap-through is predicted to occur in the phase diagram obtained from the semi-analytical model in Fig. S2B.

III. Effect of Varying Width

In these studies, we assumed that the system was constrained along the third axis, which is represented by the y -axis (that extends out of the plan of the drawing in Fig. 1). This assumption is valid for a strip is significantly wider (along y -axis) than its thickness (along the z -axis); however, in practical applications, the strip will have some finite width (along y -axis), which may have an effect on the results. The simulations of an LCE strip free to move in the xz -plane but constrained along the y -axis used to produce the plots in Fig. 1 and obtain parameters for the semi-analytical model can be repeated for a three-dimensional strip of some given width, which is free to expand along the y -axis. In this case, we modeled a strip of width $150 \text{ }\mu\text{m}$ (along y) and thickness (along z) $30 \text{ }\mu\text{m}$, for an aspect ratio of 6:1. The free strip used here has a length of $100 \text{ }\mu\text{m}$ (along x), with no constraints on the boundaries at either end. These boundary conditions will allow the material to expand along the width dimension by a greater extent than when this expansion occurs in the middle of an LCE strip clamped at both ends. Therefore, we should expect the deformation behavior of a long LCE strip undergoing a phase transition in one region to fall between this fully free system and the fully constrained system considered in Fig. 1.

We find for the three-dimensional system that the length contraction (along the axis of the nematic director) is 0.68 (ratio of initial to final length) is more pronounced than in the constrained case. The concurrent expansion along the thickness of the strip is smaller, 1.21, as it is accompanied by an equal expansion along the width. These results are displayed in Fig. S4A. Here, the length of contraction is measured along the center line of the strip parallel to the x-axis, and the change in thickness is measured over the whole height at the center of the xy-plane. The induced curvature for this strip, measured along the same line as the length contraction (Fig. S4B), follows a similar profile to that found in the constrained case (Fig. 1D), approaching an extreme value of -9.1×10^{-3} rad/ μm as intensity increases from 10 mW/cm² to 40 mW/cm² and then declining as the sample approaches a uniform level of isomerization at high intensity.

The resulting values for intensity-dependent deformation and curvature can then be substituted into our semi-analytical model to obtain a predicted phase diagram, analogous to Fig. 3. The results of this analysis are displayed in Fig. S5. Qualitatively, they are similar to those obtained in the constrained case, with the strip undergoing snap-through when the center region is exposed to light and the edges are not. Additionally, the intensity of the light must fall within a certain range to induce curvature across the thickness of the strip. If light intensity is too low to deform the material, or sufficiently high to induce comparable change in the top and bottom face, then the snap-through behavior will not occur. The phase boundary obtained from the semi-analytical method is accompanied by triangles representing finite element simulations for a three-dimensional strip of length 1 mm, thickness 30 μm and width 150 μm . The strip is held clamped at both ends, but is free to expand along the width dimension between the ends. These simulations, represented by red and blue triangles in Fig. S5, confirm that snap-through occurs for a range of aperture widths and intensities. Given the constraints at the ends of the strip, it is expected that the deformation and bending occurring in the middle of the strip will fall between that predicted by the free case (Fig. S4) and the completely constrained case (Fig. 1). As a result, we expect the observed range of parameters inducing snap through to fall between the phase boundaries predicted for these two cases, represented by dotted and dashed lines, respectively, in the figure.

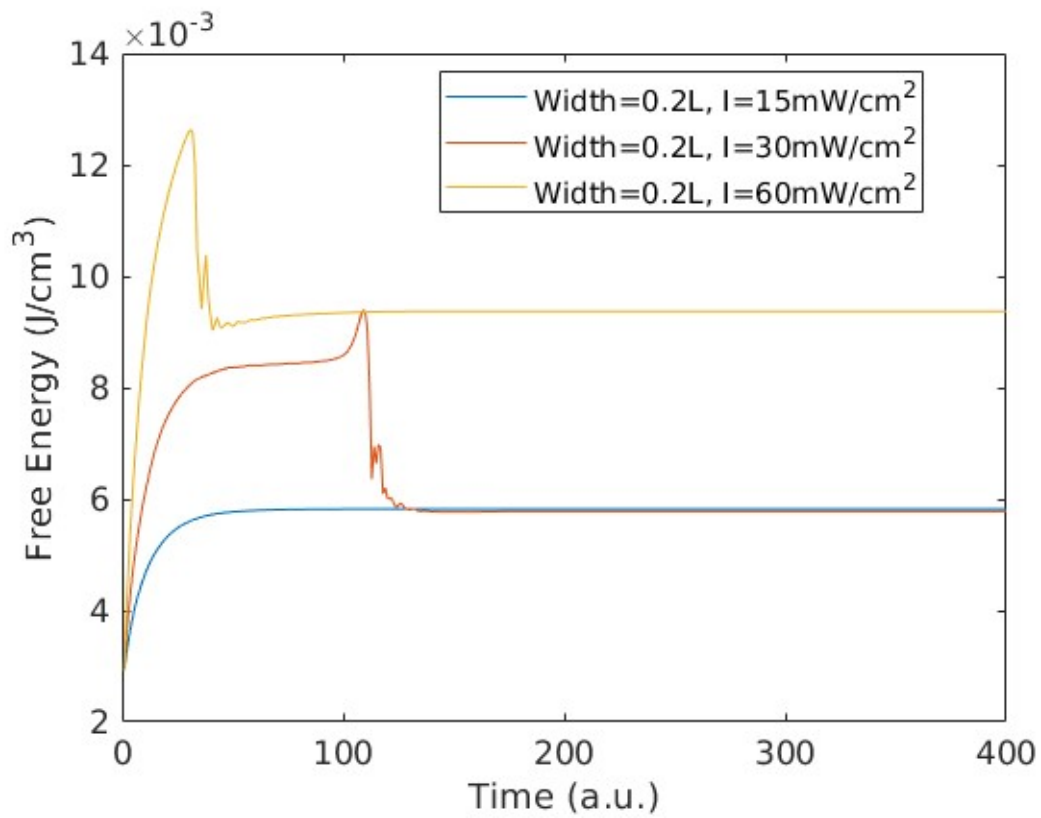


Figure S1:

Free energy vs. time. At low light (blue curve) the system deforms, but does not undergo a snap-through transition. For intermediate intensity (orange curve), the system deforms into a metastable state before transitioning to the upward buckled state. The difference between the two deformation energies (2.7 mJ/cm^3) gives an estimate of the energy released during the snap-through. For high intensity (yellow curve), the system transitions before reaching a metastable state, releasing approximately 3.3 mJ/cm^3 .

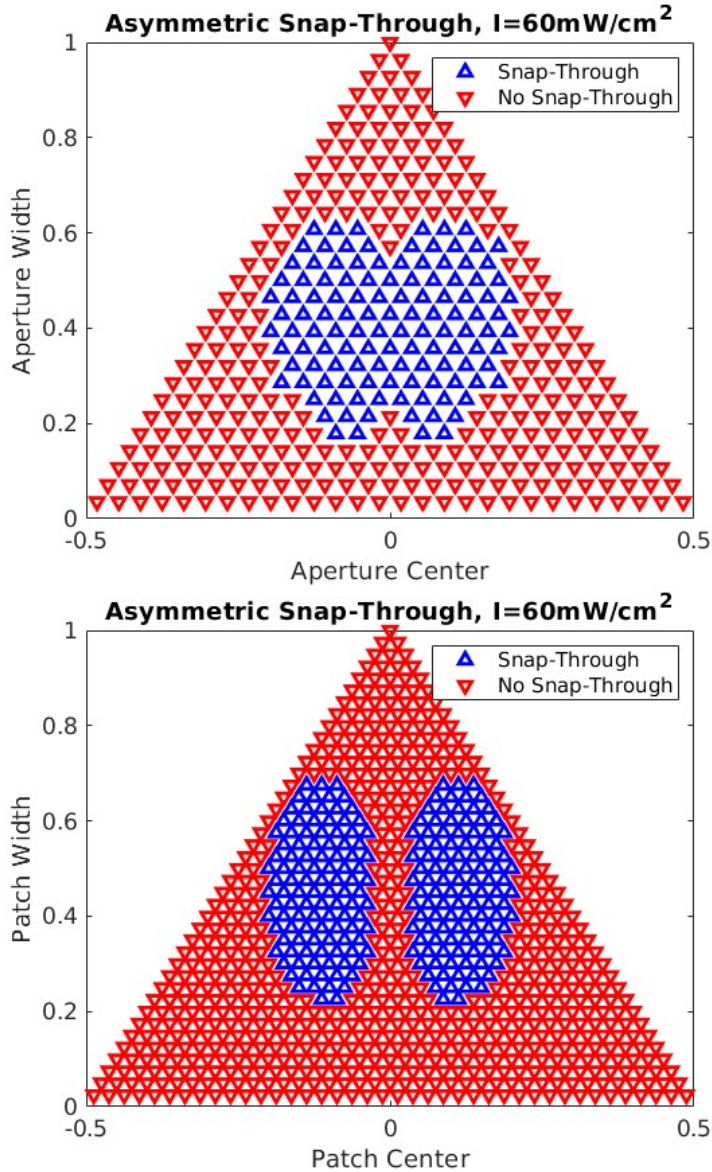


Figure S2: Phase Diagrams for Asymmetric System (A) Snap-through behavior as a function of aperture size and center position at a constant intensity of $60 \text{ mW}/\text{cm}^2$. The snap-through behavior reported in Fig. 3 for a centered aperture is robust with respect to a small displacement along the length of the strip. (B) Snap-through behavior as a function of active patch size and center position at a constant intensity of $60 \text{ mW}/\text{cm}^2$. For a centered patch, snap through fails to occur, but can be achieved with a small offset from the center of the strip.

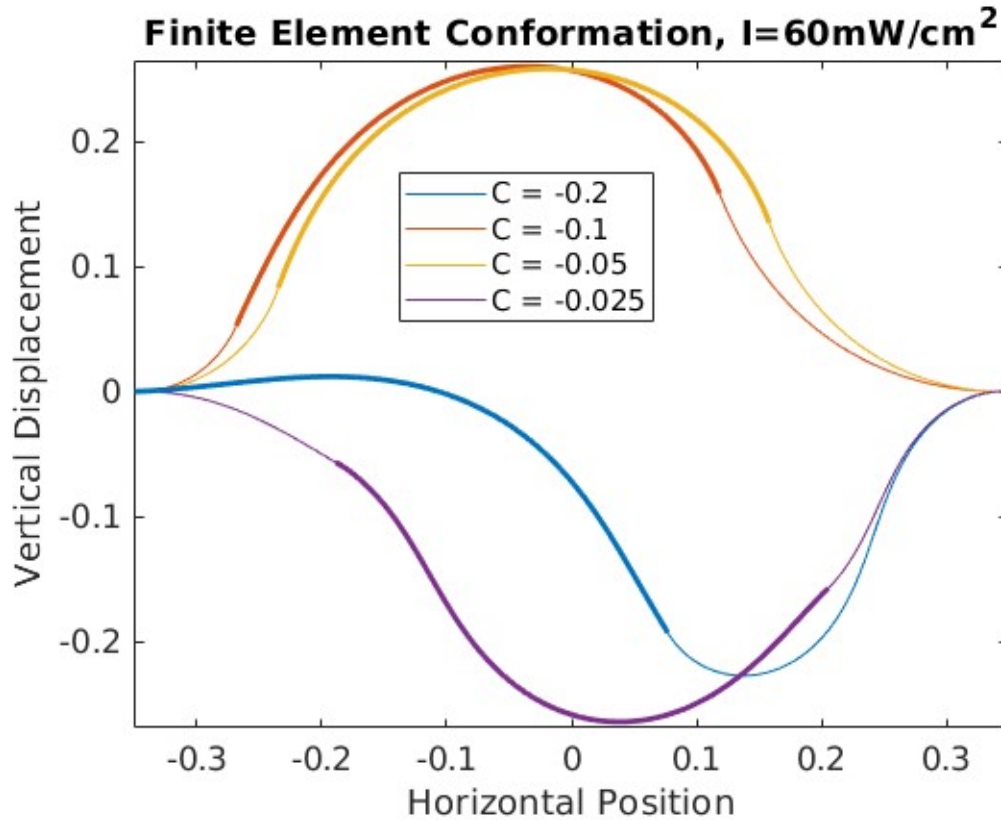


Figure S3: Finite Element Simulations for Asymmetric Patch Finite element simulations are used to corroborate the predictions of the semi-analytical model. For an active patch at the edge (blue line) or near the center (purple line) the strip remains trapped in the downward buckled state. For an active patch displaced slightly from the center transitioning from the downward buckled to upward buckled state is both energetically favorable and achievable.

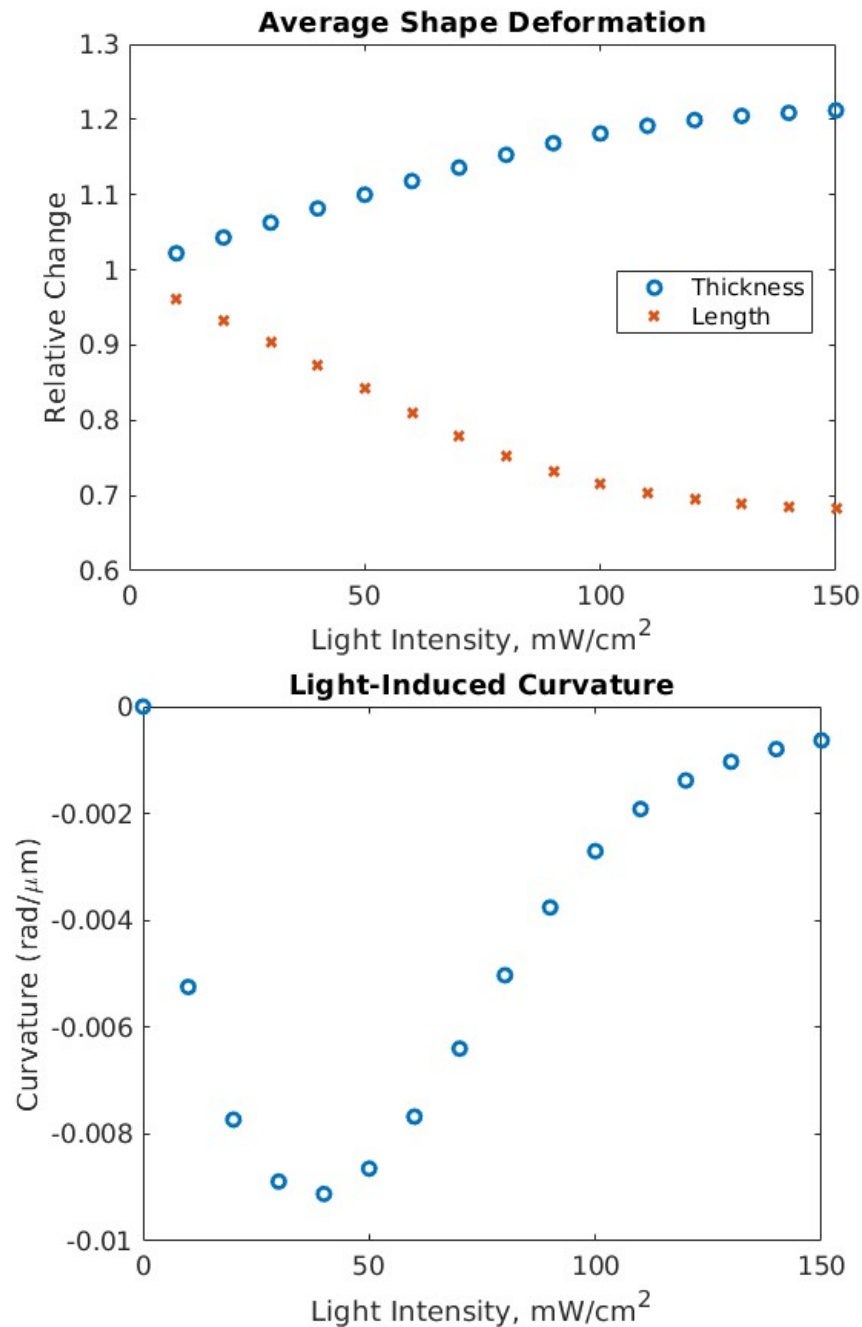


Figure S4: Deformation for 3D System. (A) Length and thickness change for free material in three dimensions. Compared to the constrained case (Fig. 1) the material undergoes a larger contraction along the director and a smaller increase in thickness. The increase in width matches the increase in thickness in this case. (B) Bending per unit length follows the same trend as in the constrained case, peaking at 40 mW/cm^2 and decreasing in magnitude as the phase change propagates through the material.

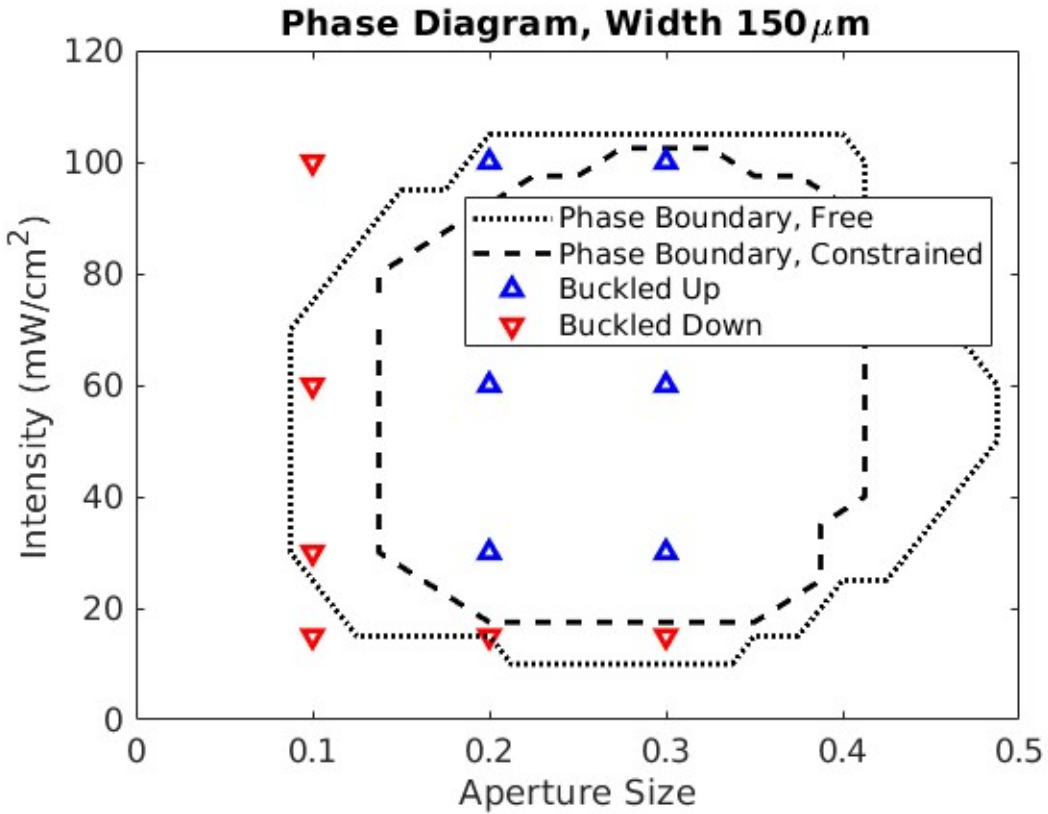


Figure S5: Phase Diagram for Finite Width Using the bending and deformation values from the free material simulations, a phase boundary is obtained for the free case (dotted line) that extends slightly beyond that found for the constrained case (dashed line). Finite element simulations with width 150 μm predict snap-through for a range of intensities and aperture sizes falling between these two curves (red and blue triangles).